

## Modeling Spatial Variability with One and Multidimensional Continuous-Lag Markov Chains<sup>1</sup>

Steven F. Carle<sup>2,3</sup> and Graham E. Fogg<sup>2,4</sup>

---

*The continuous-lag Markov chain provides a conceptually simple, mathematically compact, and theoretically powerful model of spatial variability for categorical variables. Markov chains have a long-standing record of applicability to one-dimensional (1-D) geologic data, but 2- and 3-D applications are rare. Theoretically, a multidimensional Markov chain may assume that 1-D Markov chains characterize spatial variability in all directions. Given that a 1-D continuous Markov chain can be described concisely by a transition rate matrix, this paper develops 3-D continuous-lag Markov chain models by interpolating transition rate matrices established for three principal directions, say strike, dip, and vertical. The transition rate matrix for each principal direction can be developed directly from data or indirectly by conceptual approaches. Application of Sylvester's theorem facilitates establishment of the transition rate matrix, as well as calculation of transition probabilities. The resulting 3-D continuous-lag Markov chain models then can be applied to geostatistical estimation and simulation techniques, such as indicator cokriging, disjunctive kriging, sequential indicator simulation, and simulated annealing.*

---

**KEY WORDS:** cokriging, indicator geostatistics, stochastic simulation, transition probability.

### BACKGROUND

Markov chains provide a conceptually simple and mathematically compact, yet theoretically powerful, stochastic model for categorical variables such as geologic units. Conceptually, the one-dimensional (1-D) Markov chain model applied to time series assumes that the future depends entirely upon the present and not the past. With lag replacing time for spatial applications, a 1-D Markov chain model of spatial variability assumes that a local occurrence of a category depends entirely upon the nearest occurrence of another (or the same) category, independent of more distant occurrences. Mathematically, a continuous Markov chain is a transition probability model described by a matrix exponential function (Krumbein, 1968; Agterberg, 1974, p. 457), which provides a solution to first-

<sup>1</sup>Received 19 July 1996; accepted 6 February 1997.

<sup>2</sup>Hydrologic Sciences, University of California, Davis, California 95616.

<sup>3</sup>Present address: Lawrence Livermore National Laboratory, L-206, P.O. Box 808, Livermore, California 94551. e-mail: carle1@llnl.gov

<sup>4</sup>Department of Geology, University of California, Davis, California 95616.

order stochastic (Kolmogorov) differential equations (Agterberg, 1974, p. 454–458; Ross, 1993, p. 290). In geological applications, Markov chains can be used to characterize not only random-looking patterns of spatial variability, but also relatively structured patterns involving asymmetry and cyclicity (Gingerich, 1969; Schwarzacher, 1969; Agterberg, 1974, p. 409). Theoretically, Markov chain models can be extended to 2- or 3-D spatial applications by assuming that a 1-D Markov chain characterizes spatial variability in any direction (Switzer, 1965; Lin and Harbaugh, 1984; Politis, 1994).

The usefulness of Markov chain models in geology, primarily to vertical lithologic successions, has been demonstrated convincingly for 1-D applications to quantitative interpretation and stochastic simulation, starting with the pioneering work of Vistelius (1949) followed by many other works including Carr and others (1966), Krumbein (1967), Potter and Blakely (1967), Krumbein (1968), Krumbein and Dacey (1969), Gingerich (1969), Schwarzacher (1969), Dacey and Krumbein (1970), Doveton (1971), Miall (1973), Ethier (1975), Miall (1982), Lin and Harbaugh (1984), Moss (1990), and Rolke (1991). Most of these works applied embedded Markov chains, which model successive occurrences of embedded objects, such as individual strata, independently of length. Of the remaining works, most have applied discrete-lag Markov chains, which model successive occurrences at fixed length intervals with a transition probability matrix. This paper, however, considers continuous-lag Markov chains only, which mathematically encompass discrete-lag Markov chains (Agterberg, 1974, p. 457). For purposes of stochastic simulation, continuous-lag and embedded Markov chain approaches may produce similar results, but continuous-lag Markov chains provide a more compact model of spatial variability (Harbaugh and Bonham-Carter, 1970, p. 140–149).

The suitability of the Markov chain models to 1-D geologic applications hints at potential 2- and 3-D applicability to modeling of petroleum reservoirs, aquifer systems, rock fabrics, and mineralization patterns (Doveton, 1994). Although Krumbein (1968), Lin and Harbaugh (1984), and Moss (1990) have applied Markov chain models to 2- and 3-D stochastic simulation techniques, from a mathematical standpoint, these approaches have not exploited the full potential of the multidimensional Markov chain model. A multidimensional Markov chain may include direction-dependent patterns of spatial variability that consider not only elongation of individual categories, but also juxtapositional relationships between categories. Methods for developing direction-dependent multidimensional Markov chain models have not previously emerged.

Most applications of Markov chains in geology have relied on continuous logs, a mapped stratigraphic section, or digitized patterns. In practice, exhaustive 2- or 3-D data are typically unavailable. "Hard" data, such as cores or even geophysical logs, usually are too sparse to firmly establish a model of spatial variability for nonvertical directions. Incorporation of geologic interpre-

tation may be essential to development of a geologically plausible and realistic 3-D model of spatial variability. The theoretical and conceptual simplicity of a Markov chain model provides a framework for translating subjective or semi-quantitative interpretations into a quantitative model of spatial variability. Concepts such as mean length, juxtapositional tendencies, (a)symmetry, and cyclicity (Schwarzacher, 1969) are incorporated readily into the parameters of a Markov chain model. Thus, a Markov chain model can prove useful in geology not only as an empirical model, but also as tool for quantifying a conceptual model (Vistelius, 1967; Krumbein, 1968; and Moss 1990).

Since the 1970s, however, the application of Markov chain models to geology has waned, mainly because of an absence of demonstrated applicability to 3-D problems. Attention has been shifted away from Markov theory to other geostatistical approaches that address the practical needs for grid geometry and data conditioning in 2- and 3-D estimation and stochastic simulation (e.g., Deutsch and Journel, 1992). Alternatively, indicator geostatistics can be implemented with the transition probability in lieu of the indicator (cross-)variogram (Carle and Fogg, 1996). Corresponding indicator cross-variogram, cross-covariance, or cross-correlation models can be derived easily from the transition probability. Thus, the 2- or 3-D continuous Markov chain could potentially become a useful and theoretically significant "coregionalization" model that intrinsically maintains consistency with probability laws (Ross, 1993, p. 137). Markov chain models could be used in geostatistical applications where consideration of significant spatial cross-correlations or asymmetric juxtapositional patterns, such as fining-upward tendencies (Allen, 1970b), is important. Markov chain models also could be applied to disjunctive kriging, which is theoretically equivalent to indicator cokriging (Rivoirard, 1994, p. 19). Furthermore, Markov chain models can be implemented in the simulated annealing algorithm for conditional simulation by incorporating the transition probability in the objective function (Deutsch and Journel, 1992, p. 159).

This paper presents methods for developing 1-, 2-, or 3-D continuous-lag Markov chain models, with emphasis on geostatistical applications. The 2- and 3-D Markov chain models will assume that continuous 1-D Markov chain properties exist in all directions (Switzer, 1965; Lin and Harbaugh, 1984; Politis, 1994). Thus, the development of multidimensional continuous Markov chain models relies strongly on 1-D continuous-lag Markov chain theory.

### 1-D CONTINUOUS-LAG MARKOV CHAINS

Consider a 1-D categorical dataset (e.g., lithologies in a vertical stratigraphic sequence) for which the spatial variability is assumed to be characterized by a second-order stationary model of univariate (e.g., proportions) and bivariate

(e.g., joint probability, indicator cross-covariance, transition probability) spatial statistics. The spatial variability in one direction, say  $\phi$ , may be described by a 1-D transition probability matrix  $\mathbf{T}(h_\phi)$

$$\mathbf{T}(h_\phi) = \begin{bmatrix} t_{11}(h_\phi) & \cdots & t_{1K}(h_\phi) \\ \vdots & \ddots & \vdots \\ t_{K1}(h_\phi) & \cdots & t_{KK}(h_\phi) \end{bmatrix}$$

which depends on a positive lag separation distance  $h_\phi$ , but not location  $\mathbf{x}$ . The entries  $t_{jk}(h_\phi)$  denote conditional probabilities defined as

$$t_{jk}(h_\phi) = \Pr \{(\text{category } k \text{ occurs at } \mathbf{x} + h_\phi) | (\text{category } j \text{ occurs at } \mathbf{x})\}$$

where  $j, k = 1, \dots, K$  denote mutually exclusive, exhaustively defined categories such as geologic units. The continuous-lag Markov chain model assumes that

$$\mathbf{T}(h_\phi) = \exp(\mathbf{R}_\phi h_\phi) \quad (1)$$

where  $\mathbf{R}_\phi$  is a transition rate matrix (Krumbein, 1968)

$$\mathbf{R}_\phi = \begin{bmatrix} r_{11,\phi} & \cdots & r_{1K,\phi} \\ \vdots & \ddots & \vdots \\ r_{K1,\phi} & \cdots & r_{KK,\phi} \end{bmatrix}$$

with entries  $r_{jk,\phi}$  denoting conditional rates of change per unit length from category  $j$  to category  $k$  in the direction  $\phi$ . Entries in  $\mathbf{T}(h_\phi)$  for the continuous-lag Markov chain model satisfy the Chapman-Kolmogorov relation

$$t_{jk}(h_{1,\phi} + h_{2,\phi}) = \sum_{m=1}^K t_{jm}(h_{1,\phi}) t_{mk}(h_{2,\phi}) \quad \forall j, k \quad (2)$$

for any two lags  $h_{1,\phi}$  and  $h_{2,\phi}$  positive in the direction  $\phi$  (Agterberg, 1974, p. 420; Ross, 1993, p. 266).

Although the continuous-lag Markov chain model is expressed simply and compactly in its matrix exponential form (1), the structure of each transition probability entry  $t_{jk}(h_\phi)$  consists of a linear combination of exponential functions, some of which may have complex rate coefficients indicating cyclicity. As a result, the continuous-lag Markov chain potentially can model rather complicated nonexponential-looking structures.

### Theoretical Significance

Markov chain models are significant in the context of stochastic theory. Assuming stationarity, the continuous-lag Markov chain model (1) applied in the direction  $\phi$  is the solution to the Kolmogorov forward differential equation

$$\frac{\partial}{\partial h_\phi} t_{jk}(h_\phi) = \sum_{m=1}^K t_{jm}(h_\phi) r_{mk,\phi} \quad \forall j, k \quad (3)$$

or Kolmogorov backward differential equation

$$\frac{\partial}{\partial h_\phi} t_{jk}(h_\phi) = \sum_{m=1}^K r_{jm,\phi} t_{mk}(h_\phi) \quad \forall j, k \quad (4)$$

Agterberg (1974, p. 454). These first-order stochastic differential Equations (3) and (4) reiterate that outcomes of a Markov chain model (1) in a direction  $\phi$  depend entirely on the transition rates  $r_{jk,\phi}$ . As a "first-order model" that conceptually assumes outcomes depend entirely on the closest datum, the Markov chain theoretically, is the most simple stochastic model of spatial variability for categorical variables.

Whether a first-order model is appropriate or adequate for a given application remains to be judged by the practitioner. It is possible to develop higher order Markov chains (Schwarzacher, 1969), but the resulting practical benefits may not justify the added complication, which is beyond the scope of this paper. Nonetheless, the proven applicability of first-order Markov chain models to many geologic patterns suggests that 2- or 3-D Markov chain models could be useful in geostatistical applications. Furthermore, the conceptual simplicity of the Markov chain is appealing for many practical situations where data sparseness might not support a theoretically more complicated model of spatial variability.

### Comparison to Discrete-Lag Markov Chain Models

One-dimensional Markov chain models usually are implemented in the *discrete* form in terms of a transition probability matrix  $\mathbf{T}(\Delta h_\phi)$  for a fixed lag interval  $\Delta h_\phi$ . The magnitude of  $\Delta h_\phi$  may depend rather arbitrarily on a sampling interval or data spacing. Entries in  $\mathbf{T}(i\Delta h_\phi)$  for  $i = 1, 2, \dots, \infty$  are calculated by successive application of the Chapman-Kolmogorov relation (2)

$$t_{jk}(i\Delta h_\phi) = \sum_{m=1}^K t_{jm}[(i-1)\Delta h_\phi] t_{mk}(\Delta h_\phi) \quad \forall j, k \quad (5)$$

(Ross, 1993, p. 140).

The main advantages of the continuous-lag Markov chain (1) over the

discrete approach of (5) are continuity in functional representation of the model and independence from the issue of choosing a sampling interval  $\Delta h_\phi$  (Rolke, 1991). A discrete-lag Markov chain model can be reexpressed as a continuous-lag Markov chain (1) by computing the transition rate matrix  $\mathbf{R}_\phi$  from

$$\mathbf{R}_\phi = \frac{\ln [\mathbf{T}(\Delta h_\phi)]}{\Delta h_\phi} \quad (6)$$

which enables computation of the entries  $t_{jk}(h_\phi)$  continuously for lag  $h_\phi$  by (1), not just for lag multiples of  $\Delta h_\phi$  as in (5). Note that if a pattern is characterized by a Markov chain, Equation (6) will yield the same (or similar) transition rate matrix  $\mathbf{R}_\phi$ , regardless of the selected  $\Delta h_\phi$ . Thus, the continuous-lag Markov chain provides a more general and rigorously defined model as compared to the discrete form.

For example, Figure 1 shows vertical (z)-direction transition probabilities (circles) obtained at a sampling interval of  $\Delta h_z = 0.30$  m for four types of

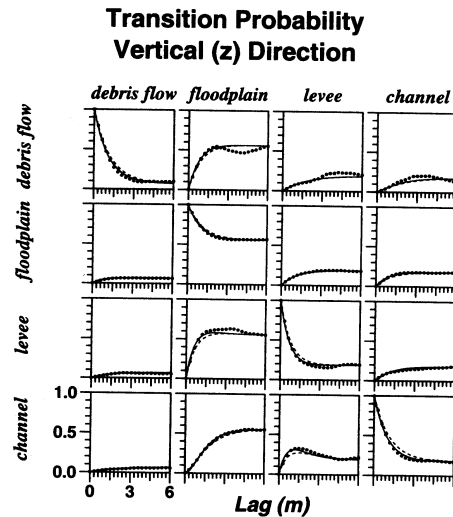


Figure 1. Transition probabilities for vertical (z) direction (dots) and Markov chain models based on  $T(\Delta h_z = 0.3$  m) and  $T(\Delta h_z = 0.9$  m) shown by dashed and solid lines, respectively.

unconsolidated alluvial sediments categorized by lithofacies

- 1 = debris flow (7%)
- 2 = floodplain (56%)
- 3 = levee (19%)
- 4 = channel (18%)

as interpreted from cores, textural descriptions, and geophysical logs obtained from vertical boreholes drilled at the Lawrence Livermore National Laboratory, Livermore, California (Qualheim, 1988; Noyes, 1990; Carle 1996), with observed proportions given in percent (%). Two continuous-lag Markov chain models were developed by applying (6) to transition probabilities at different lag intervals  $\Delta h_z$ , one for  $T(\Delta h_z = 0.30$  m) shown by dashed line, the other for  $T(\Delta h_z = 0.90$  m) shown by the solid line. Both models provide a similar fit to the transition probabilities, although the solid line provides a slightly better overall fit. In typical applications of discrete-lag Markov chains using (5), the transition probabilities for the sampling interval  $\Delta h_z = 0.30$  m would, by default, define the Markov chain model, without regard to fitting of the transition probabilities at larger lags. The larger lag transition probabilities, such as  $T(\Delta h_z = 0.90$  m) in this example, would yield an undesirably coarsely spaced model in the discrete approach (5). The continuous approach (6) provides flexibility to establish the Markov chain from transition probabilities at different magnitudes of  $\Delta h_\phi$ , while maintaining continuity in the functional representation of the model.

## PROPERTIES OF MARKOV CHAINS

### Transition Probabilities and Proportions

Consider a region  $D$  with  $K$  mutually exclusive categories. Each category  $k$  will occupy a certain volume fraction or proportion  $p_k$  in  $D$ . According to probability theory, the proportions  $p_k$  obey

$$\sum_{k=1}^K p_k = 1 \quad (8)$$

and the row sums of  $\mathbf{T}(h_\phi)$  obey

$$\sum_{k=1}^K t_{jk}(h_\phi) = 1 \quad \forall j \quad (9)$$

and the column sums of  $\mathbf{T}(h_\phi)$  obey

$$\sum_{j=1}^K p_j t_{jk}(h_\phi) = p_k \quad \forall k \quad (10)$$

where

$$0 \leq t_{jk}(h_\phi) \leq 1 \quad \forall j, k \quad (11)$$

(Ross, 1993, p. 137; Carle and Fogg, 1996). Equations (9) and (10) are instrumental for ensuring that

$$\lim_{h_\phi \rightarrow \infty} t_{jk}(h_\phi) = p_k \quad \forall j, k \quad (12)$$

as required of an ergodic Markov chain model (Ross, 1993, p. 272-274), so that local outcomes will be representative of the proportions and transition probabilities prescribed for the region  $\mathbf{D}$ . The entries in  $\mathbf{T}(h_\phi)$  also define the entries in the transition probability matrix  $\mathbf{T}(h_{-\phi})$  for the direction  $-\phi$  (opposite of  $\phi$ ) by

$$t_{jk}(h_{-\phi}) = \left( \frac{p_k}{p_j} \right) t_{kj}(h_\phi) \quad \forall j, k \quad (13)$$

#### Transition Rates

The transition rate corresponds to the slope of the transition probability as it approaches a lag of zero, as evident by differentiating (1) with respect to  $h_\phi$  at  $h_\phi = 0$

$$\frac{\partial t_{jk}(0)}{\partial h_\phi} = r_{jk,\phi} \quad \forall j, k \quad (14)$$

Applying (14) to (9) and (10) yields corresponding constraints on the row sums of  $\mathbf{R}_\phi$

$$\sum_{k=1}^K r_{jk,\phi} = 0 \quad \forall j \quad (15)$$

and column sums

$$\sum_{j=1}^K p_j r_{jk,\phi} = 0 \quad \forall k \quad (16)$$

where

$$r_{kk,\phi} \leq 0 \quad \forall k$$

and

$$r_{jk,\phi} \geq 0 \quad \forall j, k \neq j$$

(Ross, 1993, p. 267 and 273). Applying (14) to (13) yields the corresponding entries for  $\mathbf{R}_{-\phi}$  for the opposing direction  $-\phi$

$$r_{jk,-\phi} = \left( \frac{p_k}{p_j} \right) r_{kj,\phi} \quad \forall j, k \quad (17)$$

The constraints (15) and (16) are useful for ensuring that the Markov chain model satisfies (9) and (10) as required by probability law for all  $h_\phi$ . In addition, (15) and (16) ensure that the Markov chain model honors (12) with the appropriate stationary proportions  $p_k$ , which can be predetermined from conceptual information or univariate data such as the percentages given in (7). Note that (15) and (16) imply that the row and column entries of  $\mathbf{R}_\phi$  for one category, say  $\beta$ , and herein referred to as the "background" category, need not be estimated. Instead,  $r_{j\beta,\phi}$  can be calculated by

$$r_{j\beta,\phi} = - \sum_{k \neq \beta} r_{jk,\phi} \quad \forall j \neq \beta \quad (18)$$

and  $r_{\beta k}$  can be calculated by

$$r_{\beta k,\phi} = - \frac{1}{p_\beta} \sum_{j \neq \beta} p_j r_{jk,\phi} \quad \forall k \quad (19)$$

Thus, application of (18) and (19) ensures that a Markov chain model honors (12) and, using prior knowledge of proportions, requires direct specification of only  $(K-1)^2$  of the  $K^2$  entries in the transition rate matrix.

#### (A)symmetry

In some situations, juxtapositional tendencies may be assumed symmetric, eliminating the need to prescribe opposing off-diagonal entries. Let  $h_{-\phi}$  denote a lag of the same magnitude, but opposite direction of  $h_\phi$ . Assuming symmetry in the direction  $\phi$  for a transition between categories  $j$  and  $k$  indicates that  $t_{jk}(h_\phi) = t_{jk}(h_{-\phi})$  or, equivalently by applying (13)

$$t_{kj}(h_\phi) = \left( \frac{p_j}{p_k} \right) t_{jk}(h_\phi) \quad (20)$$

Applying (1) to (20) and differentiating with respect to  $h_\phi$  for  $h_\phi \rightarrow 0$ , an assumption of symmetry for transitions between categories  $j$  and  $k$  requires that

$$r_{kj,\phi} = \left( \frac{p_j}{p_k} \right) r_{jk,\phi} \quad (21)$$

Equation (21) provides an important tool during model development because if symmetry in juxtapositional tendencies is assumed for categories  $j$  and  $k$ , then establishment of one transition rate  $r_{jk, \phi}$  establishes the opposing transition rate  $r_{kj, \phi}$ , or vice versa. From an interpretive standpoint, symmetry would be assumed for a direction in which the pattern of heterogeneity does not change when viewed by the opposite direction. For example, if symmetric juxtapositional patterns of ABCBA tend to occur one direction, then the same ABCBA tendency would persist in the opposing direction. However, if an asymmetric ABCABC pattern tends to occur in one direction, that tendency would occur as CBACBA in the opposing direction. Most indicator geostatistical models intrinsically assume symmetry by quantifying spatial variability with the indicator (cross-)variogram, which is symmetric by definition. However, asymmetric patterns are not unusual in geology, particularly in vertical lithologic successions (Schwarzacher, 1969). Consequently, the transition probability is more appropriate than the indicator (cross-)variogram for certain geological applications.

#### Sparse Data

Most applications of Markov chains to geology have applied the discrete approach (5) to "continuous" data such as vertical stratigraphic sequences or continuously logged core. However, geologic data are seldom adequately numerous and closely spaced in nonvertical directions to apply directly a discrete-lag Markov chain model. For example, Figure 2 shows strike ( $x$ )-direction transition probabilities sampled at an interval of 3 m for the same dataset described in Figure 1. Most of the boreholes are spaced farther apart than the mean strike-direction lengths of the lithofacies categories. Consequently, far fewer data are available to evaluate strike-direction spatial variability as compared to the vertical. This problem hampers application of geostatistics to subsurface datasets.

Uncertainty in the transition probability data does not favor direct application of (6) to formulate a continuous-lag Markov chain model. In Figure 2, for example,  $T(\Delta h_x = 3 \text{ m})$  and  $T(\Delta h_x = 9 \text{ m})$  applied to (6) yield Markov chain models shown by the dashed and dotted lines, respectively. Note that the sills for these two models are slightly different because different proportions are associated with a limited number of data pairs used to estimate  $T(\Delta h_x = 3 \text{ m})$  and  $T(\Delta h_x = 9 \text{ m})$ ; the proportions  $p_k$  determined by the entire dataset are more likely a better indicator of an appropriate model sill according to (12). Furthermore, if a transition probability for the selected lag interval is errant or inconsistent with other transition probabilities at other lags, for example,  $t_{12}(\Delta h_x = 9 \text{ m})$  for the debris flow  $\rightarrow$  floodplain transition in Figure 2, the resulting model will not be representative of the overall trend of the data. Thus, given uncertain

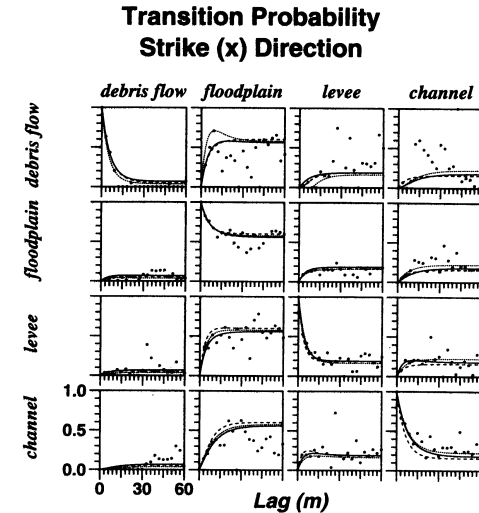


Figure 2. Transition probabilities for strike ( $x$ ) direction (dots) and Markov chain models based on  $T(\Delta h_x = 3 \text{ m})$  and  $T(\Delta h_x = 9 \text{ m})$  shown by dashed and dotted lines, respectively; Markov chain model developed by fitting transition rates shown by solid line.

transition probability data, no single transition probability matrix for a particular lag is likely to yield a fully satisfactory Markov chain model.

Alternatively, one can develop a 1-D continuous-lag Markov chain model by "fitting"  $(K - 1)^2$  of the  $K^2$  transition rates in conjunction with an *a priori* assumption for the proportions based on the entire dataset. Note that (14) implies that  $r_{jk, \phi}$  can be established from the slope of  $t_{jk}(h_\phi)$  at  $h_\phi = 0$ . Thus, instead of focusing on a transition probability matrix for one particular lag, one can develop the model from (1) by fitting transition rates  $r_{jk, \phi}$  to estimates of  $\partial t_{jk}(0)/\partial h_\phi$  exhibited by the trend of the transition probabilities as  $h_\phi \rightarrow 0$ . Application of (15) or (18) determines the transition rate of one entry given the other  $K - 1$  entries along a row. The assumed proportions can be applied with (16) or (19) to obtain one entry from the remaining  $K - 1$  entries along a column. The resulting model will obey (12) with sills that correspond to the measured or assumed proportions.

For example, a rate-fitting approach was used to develop a continuous-lag

Markov chain model, shown in Figure 2 by the solid line, from (1) with category 2 (floodplain) assumed as background. The rate matrix  $\mathbf{R}_x$  for the strike ( $x$ ) direction was developed as

$$\mathbf{R}_x = \begin{bmatrix} -0.16 & c_1 & s & s \\ c_2 & c_2 & c_2 & c_2 \\ 0.010 & c_1 & -0.20 & s \\ 0.002 & c_1 & 0.07 & -0.11 \end{bmatrix} \text{m}^{-1} \quad (22)$$

where “ $c_1$ ” denotes the row-sum constraint of (15) or (18), “ $c_2$ ” denotes the column-sum constraint of (16) or (19), and “ $s$ ” denotes a symmetry assumption (21). Note that in this example, only 6 of the 16 rate coefficients needed direct specification by fitting of  $\partial t_{jk}(0)/\partial h_\phi$ . The resulting continuous Markov chain model provides good overall fit to the strike-direction transition probabilities, and the sills (or stationary proportions) are consistent with proportions given in (7).

### CONCEPTUAL DEVELOPMENT

Clearly, the development of a continuous-lag Markov chain model, whether directly from  $\mathbf{T}(\Delta h_\phi)$  by applying (6) or indirectly by fitting  $\partial t_{jk}(0)/\partial h_\phi$ , relies on establishing the transition rate matrix  $\mathbf{R}_\phi$ . In addition,  $\mathbf{R}_\phi$  can be developed from conceptual information, thus enabling the use of geologic interpretation in developing Markov chain models.

In many subsurface investigations, particularly those relying on vertical boreholes as control, the data are insufficient to empirically establish a spatial variability model in all but the vertical direction. Even if data are relatively abundant and closely spaced in nonvertical directions, the effects of unknown variations in dip and strike can rarely be accounted for. Thus, geologic interpretation usually must intervene in model building because a purely empirical approach overlooks valuable subjective geologic information. A conceptual understanding of the transition rate matrix can be used to develop Markov chain models from interpretations of proportion, mean length, juxtapositional tendencies, and (a)symmetry. Such understanding also helps ensure geologic plausibility during model development whether data are abundant or sparse.

#### The Background Category

In applying (18) and (19) to development of a transition rate matrix, it may be useful to conceive of the “background category”  $\beta$  as the category that

“fills” in the remaining space not occupied by other categories. For example, in modeling a mineralization pattern, the last mineral to form or a nonmineralized zone would be a logical selection for a background category. In modeling a fluvial depositional system, a floodplain depositional unit would tend to occupy the remaining accommodation space not taken up by the units formed by higher energy depositional processes and, consequently, would be a logical choice for background category. Thus, from a conceptual viewpoint the choice of background category is usually clear. However, from the mathematical viewpoint of (18) and (19), any category can be selected as a background category.

#### Mean Length

The mean length  $\bar{L}_{k,\phi}$  of a category  $k$  along lines in the direction  $\phi$  is the total length occupied by category  $k$  divided by the number of embedded occurrences of  $k$ . For example, mean length for the vertical direction corresponds to the more widely used term of “mean thickness.” Given that

$$\frac{\partial t_{kk}(0)}{\partial h_\phi} = -\frac{1}{\bar{L}_{k,\phi}} \quad (23)$$

(Carle and Fogg, 1996), applying (14) to (23) yields

$$r_{kk,\phi} = -\frac{1}{\bar{L}_{k,\phi}} \quad (24)$$

Thus, a plausible estimate of  $\bar{L}_{k,\phi}$  can be used in expression (24) to specify the diagonal entries  $r_{kk,\phi}$  in the transition rate matrix for a Markov chain model.

For the two-category ( $K = 2$ ) situation, the mean length in a direction  $\phi$  relates to the “effective range” of “ $3a_\phi$ ” traditionally used in geostatistics for an exponential structure (Deutsch and Journel, 1992, p. 23) by

$$\bar{L}_{k,\phi} = \frac{a_\phi}{1 - p_k}$$

However, for  $K \geq 3$  each entry of the Markov chain becomes a sum of two or more exponential structures, which also may involve complex rate coefficients. Thus, compared to mean length, a “range” parameter becomes more difficult to directly incorporate into conceptual development of Markov chain models.

#### Juxtapositional Tendencies

The off-diagonal transition rates prescribe the juxtapositional tendencies, that is the probabilities at which embedded occurrences of different categories occur adjacent to each other. A significant reason that *embedded* Markov chain analyses have been applied to geologic data is to examine how off-diagonal

transitions deviate, if at all, from various reference states such as maximum entropy (disorder) or independent (random) juxtapositional tendencies. Thus, a transition rate  $r_{jk,\phi}$  could be interpreted relative to  $r_{jk,\phi}^*$ , a transition rate for a particular reference state, by

$$r_{jk,\phi} = a_{jk,\phi}(r_{jk,\phi}^*) \quad \text{for } k \neq j \quad (25)$$

where  $a_{jk,\phi}$  denotes a positive coefficient. For example, assuming that  $a_{jk,\phi} = 2.0$  would constitute a transition rate of two times greater than the reference state.

Juxtapositional tendencies have been interpreted relative to entropy of transition probabilities of embedded occurrences (Hattori, 1976), proportions of transition probabilities (Carle and Fogg, 1996), numbers of embedded occurrences (Miall, 1973; Miall, 1982), or transition frequencies of embedded occurrences (Goodman, 1968; Turk, Naylor, and Woodcock, 1979). The following derivations show how these models also could be applied to continuous-lag Markov chain models in terms of proportions, mean lengths, and transition rates.

### Entropy

The entropy  $E_j$  of juxtapositional tendencies in terms of transition probabilities of embedded occurrences in a direction  $\phi$  is measured by

$$E_{j,\phi} = - \sum_{k=1}^K \tau_{jk,\phi} \ln [\tau_{jk,\phi}]$$

where  $\tau_{jk,\phi}$  is defined as

$\tau_{jk,\phi} = \Pr \{k \text{ is juxtaposed to } j \text{ in the direction } \phi \mid \text{an embedded occurrence of } j\}$

Hattori (1976). Recognizing by (15) and (24) that  $\tau_{jk,\phi}$  also can be defined in terms of transition rates and mean length by

$$\tau_{jk,\phi} = \frac{r_{jk,\phi}}{-r_{jj,\phi}} = \bar{L}_{j,\phi} r_{jk,\phi}$$

the entropy also could be measured in the framework of a continuous-lag Markov chain analysis by

$$E_{j,\phi} = - \sum_{k=1}^K \bar{L}_{j,\phi} r_{jk,\phi} \ln [\bar{L}_{j,\phi} r_{jk,\phi}]$$

A transition rate matrix with entries  $r_{jk,\phi}^*$  corresponding to a reference state of maximum entropy (disorder) then could be derived by maximizing  $\sum_{j=1}^K E_{j,\phi}$  subject to (15) and (16) and assumed mean lengths.

### Proportions of Auto-Transition Rate

If  $\Pr\{k \neq j \text{ occurs at } x + h_\phi \mid j \text{ occurs at } x\}$  is assumed to depend on category proportions  $p_k$ , then off-diagonal transition probabilities  $t_{jk}^*(h_\phi)$  referenced with respect to  $p_k$  would be calculated by

$$t_{jk}^*(h_\phi) = [1 - t_{jj}(h_\phi)] \frac{p_k}{1 - p_j} \quad \text{for } k \neq j \quad (26)$$

(Carle and Fogg, 1996). Differentiating (26) with respect to  $h_\phi$  at  $h_\phi = 0$ , corresponding off-diagonal transition rates  $r_{jk,\phi}^*$  referenced to proportions would be

$$r_{jk,\phi}^* = -r_{jj,\phi} \frac{p_k}{1 - p_j} \quad \text{for } k \neq j \quad (27)$$

### Numbers of Embedded Occurrences

In an embedded Markov chain analysis (Krumbein and Dacey, 1969), the "transition counts" or frequencies  $f_{jk,\phi}$  of transitions between embedded occurrences of  $j$  to  $k \neq j$  in the direction  $\phi$  are considered, irrespective of the lengths of the embedded occurrences. Defining  $s_{k,\phi} = \sum_{j=1}^K f_{jk,\phi}$  as the number of embedded occurrences of  $k$  along lines in the direction  $\phi$ , the conditional probability  $q_{jk,\phi}^*$  that a transition occurs according to the numbers of embedded occurrences is determined by

$$q_{jk,\phi}^* = \frac{s_{k,\phi}}{\sum_{m \neq j} s_{m,\phi}} \quad (28)$$

(Miall, 1973, 1982). Considering that  $s_{k,\phi} \propto p_k \bar{L}_{k,\phi}$  (Carle and Fogg, 1996) and applying  $r_{jj,\phi} = -\sum_{k \neq j} r_{jk,\phi}$  and  $1 = \sum_{k \neq j} q_{jk,\phi}^*$ , then transition rates  $r_{jk,\phi}^*$  referenced to the numbers of embedded occurrences can be established by

$$r_{jk,\phi}^* = -r_{jj,\phi} \frac{\frac{p_k}{\bar{L}_{k,\phi}}}{\sum_{m \neq j} \frac{p_m}{\bar{L}_{m,\phi}}} \quad (29)$$

where  $\bar{L}_{k,\phi}$  denotes mean length.

### Transition Frequencies of Embedded Occurrences

One noticeable deficiency in the previous two methods as described for establishing what could be construed as "random" transition rates is the lack

of symmetry in accordance with (21), which would be expected in truly random juxtapositional relationships. This point has been brought to attention by Turk (1982) and Turk, Naylor, and Woodcock (1979), who suggests that "random" juxtapositional relationships should be defined according to independence of transition frequencies of embedded occurrences including the "unobservable" self-transitions. Let  $f_{j,\phi}$  denote the frequency of embedded occurrences of  $j$  in the direction  $\phi$  and  $f_{jk,\phi}$ , correspondingly, the frequency of transitions from  $j$  to  $k$ , including the possibility for self-transitions  $f_{jj,\phi}$ . The entries  $f_{jk,\phi}^*$  of an independent transition frequency matrix will obey

$$f_{jk,\phi}^* = f_{j,\phi} f_{k,\phi} \quad \forall j, k = 1, \dots, K \quad (30)$$

Because self-transitions are unobservable, only the off-diagonal transition frequencies can be observed. The problem of determining independent juxtapositional relationships is to find  $f_{j,\phi}$  which satisfy (30) while obeying the observed off-diagonal row/column totals  $s_{j,\phi}$

$$s_{j,\phi} = \sum_{k \neq j}^K f_{jk,\phi} \quad \forall j = 1, \dots, K \quad (31)$$

which are related to proportions and mean length by

$$s_{j,\phi} \propto \frac{p_j}{L_{j,\phi}} \quad \forall j = 1, \dots, K$$

An iterative scheme analogous to iterative proportion fitting (Goodman, 1968) can be devised to satisfy (15) and (16) as follows:

1. Initialize  $f_{j,\phi}$  with  $s_{j,\phi}$ .
2. Estimate  $f_{jk,\phi}^*$  by applying (30).
3. Estimate  $f_{j,\phi}$  by  $f_{j,\phi} = s_{j,\phi} / \sum_{k \neq j}^K f_{jk,\phi}^*$  to maintain consistency with (31).
4. Repeat steps 2 and 3 until convergence.

The independent transition frequencies can be translated to "independent" transition rates  $r_{jk,\phi}^*$  consistent with observed proportions and mean lengths by

$$r_{jk,\phi}^* = -\frac{1}{L_{j,\phi}} \left( \frac{f_{jk,\phi}^*}{s_{j,\phi}} \right)$$

### Example

The lithofacies data used in the previous examples to assess the vertical- and strike-direction spatial variability were inadequate to assess dip-direction

spatial variability. This was the result of not only a shortage of lag pairs, but because of unknown subsurface variations in azimuthal and dip directions of the alluvial deposits, which have a profound impact on measuring spatial variability in the direction of greatest elongation (the dip direction). Rather than force-fitting a model to inadequate data, a dip model of spatial variability could be synthesized aided by geologic interpretation.

For example, the juxtapositional tendencies for the dip direction may be assumed similar to those for the strike direction, but with different mean lengths for each category. Applying (25) to (27), the strike ( $x$ ) direction transition rate matrix (22) could be viewed as

$$\mathbf{R}_x = \begin{bmatrix} -\frac{1}{6.25} & c_1 & s & s \\ c_2 & c_2 & c_2 & c_2 \\ 0.58r_{31,x}^* & c_1 & -\frac{1}{5.0} & s \\ 0.22r_{41,x}^* & c_1 & 2.8r_{43,x}^* & -\frac{1}{9.00} \end{bmatrix} \text{m}^{-1} \quad (32)$$

where the denominators in diagonal entries  $r_{kk,x}$  represent the mean length  $\bar{L}_{k,x}$  of category  $k$  in the  $x$  direction according to (24), and the  $r_{jk,x}^*$  terms in the off-diagonal entries are referenced, in this situation, with respect to proportions of the autotransition rates by (27). Note that the reference state model (27) generally is easier to apply than either (31), (29), or the entropy concept because it does not require an input for the mean length of a background category. Based on geologic interpretation, dip:strike anisotropy ratios of 4:1 for debris flow lobes, 8:1 for channel stringers, and 6:1 for levee deposits were assumed, which yield dip ( $y$ )-direction mean lengths  $\bar{L}_{k,y}$  of 25 m, 30 m, and 72 m for categories 1, 3, and 4, respectively. Assuming similar juxtapositional tendencies for both the dip direction and the strike direction, as established by (32), a dip ( $y$ )-direct transition rate matrix can be obtained from

$$\mathbf{R}_y = \begin{bmatrix} -\frac{1}{25} & c_1 & s & s \\ c_2 & c_2 & c_2 & c_2 \\ 0.58r_{31,y}^* & c_1 & -\frac{1}{30.0} & s \\ 0.22r_{41,y}^* & c_1 & 2.8r_{43,y}^* & -\frac{1}{72.00} \end{bmatrix} \text{m}^{-1}$$

where, again,  $r_{jk,y}^*$  would be referenced to (27), but with respect to the y-direction autotransition rates. The resulting transition probability model for the dip (y) direction is shown in Figure 3.

Clearly, alternative interpretations could have been made to develop the dip-direction rate matrix. For example, an interpretation of Walther's Law, that vertical successions represent the lateral succession of environments of deposition (Leeder, 1982, p. 122; Doveton, 1994), might incorporate the fining-upward asymmetry seen in vertical-direction transition rates to establish a fining-outward asymmetry in the dip-direction transition rates.

The coefficients in (25) mainly serve as a tool for establishing off-diagonal entries for  $R_\phi$  that are interpreted more easily than the actual numerical values. Thus, the patterns of heterogeneity implied by the rate coefficients can be evaluated empirically by generating 3-D stochastic simulations from the Markov chain models (Carle, 1996). If the resulting stochastic simulations do not yield expected or desired patterns, the entries in the rate matrices can be adjusted accordingly.

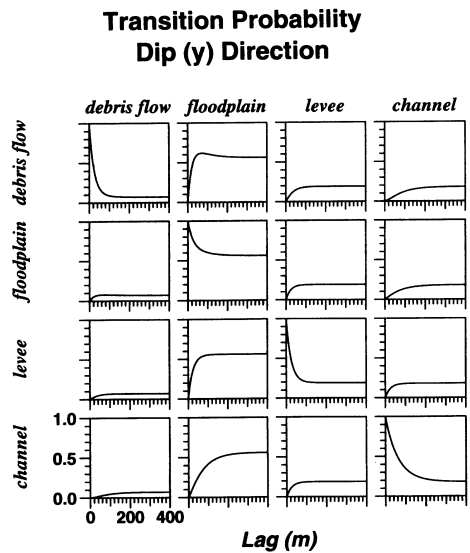


Figure 3. Markov chain model for dip (y) direction developed by rescaling strike-direction model.

**SYLVESTER'S THEOREM**

Sylvester's theorem provides a rapid, direct method for calculating polynomials of a matrix (Agterberg, 1974, p. 406-409), which can be extended to the determination of the entries in a 1-D continuous-lag Markov chain (1) established by transition rates or transition probabilities at a discrete lag. Equations (1) and (6) involve matrix exponentials and matrix logarithms, respectively, which can be evaluated in canonical form (Agterberg, 1974, p. 85), by power series (Agterberg, 1974, p. 406), or, more directly, by applying Sylvester's theorem (Agterberg, 1974, p. 412, p. 457).

The transition rate matrix  $R_\phi$  can be expressed as

$$R_\phi = \sum_{l=1}^K \lambda_{l,\phi} Z_{l,\phi} \tag{33}$$

where the  $\lambda_{l,\phi}$  are the  $l = 1, \dots, K$  eigenvalues of  $R_\phi$ , and  $Z_{l,\phi}$  is a spectral component matrix associated with each  $\lambda_{l,\phi}$ . The  $Z_{l,\phi}$  are computed by

$$Z_{l,\phi} = \frac{\prod_{i \neq l} (\lambda_{i,\phi} \mathbf{I} - R_\phi)}{\prod_{i \neq l} (\lambda_{i,\phi} - \lambda_{l,\phi})} \quad \forall l = 1, \dots, K \tag{34}$$

where  $\mathbf{I}$  represents the identity matrix. Application of Sylvester's theorem to the power-series representation of a continuous-lag Markov chain model (1) yields

$$T(h_\phi) = \exp(R_\phi h_\phi) = \sum_{l=1}^K \exp(\lambda_{l,\phi} h_\phi) Z_{l,\phi} \tag{35}$$

(Agterberg, 1974, p. 412, p. 457). Thus, for a Markov chain model, the eigenvalues  $\theta_l(h_\phi)$ ,  $l = 1, \dots, K$  of  $T(h_\phi)$  relate to the eigenvalues of  $R_\phi$  by

$$\theta_l(h_\phi) = \exp(\lambda_{l,\phi} h_\phi) \quad \forall l = 1, \dots, K$$

or

$$\lambda_{l,\phi} = \frac{\ln \theta_l(h_\phi)}{h_\phi} \quad \forall l = 1, \dots, K \tag{36}$$

Furthermore, the entries  $z_{jk,l,\phi}$  in  $Z_{l,\phi}$  obtained from  $T(h_\phi)$  by

$$\mathbf{Z}_{l,\phi} = \frac{\prod_{i \neq l} [\theta_i(h_\phi) \mathbf{I} - \mathbf{T}(h_\phi)]}{\prod_{i \neq l} [\theta_i(h_\phi) - \theta_i(h_\phi)]} \quad \forall l = 1, \dots, K \quad (37)$$

are identical to those defined for  $\mathbf{R}_\phi$  in (34).

Under the assumption of a Markov chain model of spatial variability,  $\mathbf{T}(\Delta h_\phi)$  for a discrete lag interval  $\Delta h_\phi$  can be used to establish  $\mathbf{R}_\phi$  by finding the eigenvalues  $\theta_l(\Delta h_\phi)$  corresponding to  $\mathbf{T}(\Delta h_\phi)$  and applying (36) and (37) to obtain

$$\mathbf{R}_\phi = \sum_{l=1}^K \frac{\ln \theta_l(\Delta h_\phi)}{\Delta h_\phi} \mathbf{Z}_{l,\phi} \quad (38)$$

Application of (38) to (1) yields a continuous-lag Markov chain model based on  $\mathbf{T}(\Delta h_\phi)$

$$\mathbf{T}(h_\phi) = \sum_{l=1}^K \theta_l(\Delta h_\phi)^{h_\phi/\Delta h_\phi} \mathbf{Z}_{l,\phi} \quad (39)$$

which represents, in effect, a continuous version of the more widely used discrete-lag Markov chain model (5).

Note in (35) that a 1-D continuous-lag Markov chain model can be viewed as a linear combination of exponential functions  $\theta_l(h_\phi)$ . Nonnegative definiteness can be satisfied if the  $\mathbf{Z}_{l,\phi}$  matrices and  $\exp(\lambda_{l,\phi} h_\phi)$  functions are nonnegative definite, thus conforming to a "linear model of coregionalization" (Journel and Huijbregts, 1978, p. 171; Goulard and Voltz, 1992; Goovaerts, 1994).

The largest eigenvalue of  $\mathbf{T}(h_\phi)$ , say  $\theta_1(h_\phi)$ , should be equal to unity to ensure compliance with (8) and (12). The corresponding entries for the spectral component matrix for  $\theta_1(h_\phi)$  will be  $z_{jk,1,\phi} = p_k$ , where  $p_k$  are the stationary proportions intrinsic to  $\mathbf{T}(h_\phi \rightarrow \infty)$ . Considering (36), the eigenvalue  $\lambda_1$  for  $\mathbf{R}_\phi$  should be zero. Some eigenvalues  $\theta_l(h_\phi)$  of  $\mathbf{T}(h_\phi)$  may be complex, forming conjugate pairs if cyclicity exists in the model. However, the real part should be nonnegative but less than unity to ensure compliance with (11). Correspondingly, the real part of the remaining eigenvalues  $\lambda_{l,\phi}$  for  $\mathbf{R}_\phi$  should be negative. Nonnegative eigenvalues for  $\mathbf{T}(h_\phi)$  maintain nonnegative-definiteness and avoid undefined values for the eigenvalues of  $\mathbf{R}_\phi$ .

In practice, either the eigenvalues  $\lambda_{l,\phi}$  or  $\theta_l(h_\phi)$  corresponding to the real general matrices  $\mathbf{R}_\phi$  or  $\mathbf{T}(h_\phi)$ , respectively, can be computed from FORTRAN subroutines given by Smith and others (1976) or Press and others (1992). The

spectral matrices  $\mathbf{Z}_{l,\phi}$  then are computed by applying (34) or (37), and the continuous-lag Markov chain model of  $\mathbf{T}(h_\phi)$  is computed from (35) or (39).

### EXTENSION TO 3-D

The extension of Markov chain models to 2- and 3-D applications may rely on an assumption that spatial variability along any direction can be modeled by a Markov chain, in accordance with Switzer's (1965) theorem and the definition of a multidimensional Markov chain given by Politis (1994). Each 1-D Markov chain model for each of the infinity of directions may differ, as long as the assumed category proportions remain constant. However, subsurface data usually will be insufficient to develop a multidimensional Markov chain model for an infinity of directions. Alternatively, development of a 3-D continuous Markov chain model can focus on establishing 1-D Markov chain models for each of three principal directions, say strike, dip, and vertical (upward) or stratigraphic  $x$ ,  $y$ , and  $z$ . Then, 1-D Markov chain models for any direction can be established by interpolation from the principal-direction models. The resulting 3-D Markov chain models may consider different juxtapositional tendencies in different directions as established from the principal-direction models using the purely quantitative, semiquantitative, or conceptual approaches previously described in this paper.

The key to development of a 1-D continuous-lag Markov chain model for a direction  $\phi$  has been establishment of the transition rate matrix  $\mathbf{R}_\phi$ . Similarly, the key to interpolating 1-D Markov chain models to arbitrary directions will be determined through interpolation of the principal-direction transition rate matrices,  $\mathbf{R}_x$ ,  $\mathbf{R}_y$ , and  $\mathbf{R}_z$ . At first glance, it might seem more intuitive to establish a 3-D Markov chain model by ellipsoidally interpolating the transition probability matrices  $\mathbf{T}(h_x)$ ,  $\mathbf{T}(h_y)$ , and  $\mathbf{T}(h_z)$ . However, examples later will show that nonellipsoidal transition probability model structures may exist in association with asymmetric juxtapositional relationships.

### Interpolation Scheme

The interpolation scheme for developing a 3-D Markov chain model requires that 1-D Markov chain models for the principal  $x$ ,  $y$ , and  $z$  directions be established, with each model assuming the same stationary proportions. To interpolate the transition probability matrix  $\mathbf{T}(h_x, h_y, h_z)$  for an arbitrary direction  $\phi$ , one category  $\beta$  is selected as "background," and entries in the transition rate matrix  $\mathbf{R}_\phi$  are interpolated ellipsoidally by

$$|r_{jk,\phi}| = \sqrt{\left(\frac{h_x}{h_\phi} r_{jk,x}\right)^2 + \left(\frac{h_y}{h_\phi} r_{jk,y}\right)^2 + \left(\frac{h_z}{h_\phi} r_{jk,z}\right)^2}$$

$\forall j \neq \beta, k \neq \beta$  (40)

where  $h_\phi = \sqrt{h_x^2 + h_y^2 + h_z^2}$ . If any of the lag vector components  $h_x$ ,  $h_y$ , or  $h_z$  are negative, then entries  $r_{jk,-x}$ ,  $r_{jk,-y}$ , or  $r_{jk,-z}$  as computed by (17), respectively, are used in (40). Equations (18) and (19) are used to complete the row and column entries  $r_{j\beta,\phi}$  or  $r_{\beta k,\phi}$  for  $j, k = 1, \dots, K$ .

To compute the Markov chain model of  $\mathbf{T}(h_x, h_y, h_z)$  by (1), the eigenvalues of  $\mathbf{R}_\phi$  are determined, then the spectral components are computed by (34), and, finally, (35) is applied for  $h_\phi = \sqrt{h_x^2 + h_y^2 + h_z^2}$ .

**Example**

A 3-D Markov chain model was developed from the vertical ( $z$ ), strike ( $x$ ), and dip ( $y$ ) direction 1-D Markov chain models given in Figures 1, 2, and 3, respectively. The 3-D transition probability matrices are difficult, if not impossible, to display graphically. However, a suite of 2-D slices through the 3-D models shown in Figures 4, 5, and 6 illustrate the juxtapositional tendencies

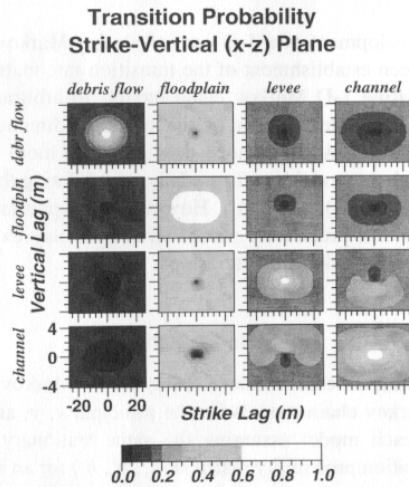


Figure 4. Slice from strike-vertical ( $x - z$ ) plane of a 3-D Markov chain model interpolated from 1-D Markov chain models developed for the strike, dip, and vertical directions.

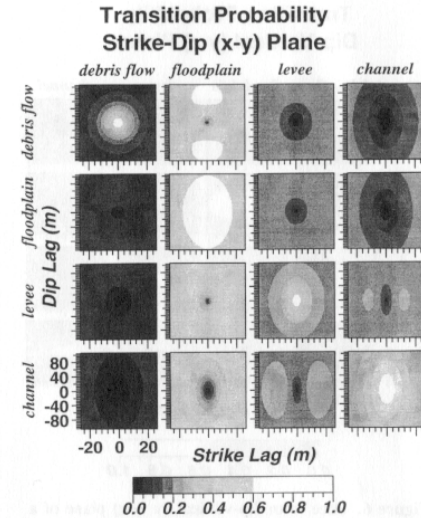


Figure 5. Slice from strike-dip ( $x - y$ ) plane of a 3-D Markov chain model.

established by the 1-D vertical, strike, and dip models through either purely quantitative, semiquantitative, and conceptual methods.

Figure 4 shows a slice through the 3-D model at  $y = 0$ , which, in effect, shows a 2-D Markov chain model for the vertical-strike ( $x - z$ ) plane. The diagonal transition probabilities  $t_{kk}(t_\phi)$  are symmetric because (13) reduces to

$$t_{kk}(h_{-\phi}) = t_{kk}(h_\phi)$$

when  $j = k$ . However, the off-diagonal transition probabilities  $t_{jk}(h_\phi)$  for  $j \neq k$  are not necessarily ellipsoidally symmetric because of asymmetric juxtapositional relationships.

The off-diagonal transition probabilities  $t_{jk}(h_x, 0, h_z)$  in the strike-vertical ( $x - z$ ) model of Figure 4 are clearly asymmetric with respect to the vertical ( $z$ ) direction, especially for the  $3 \rightarrow 4$  (levee  $\rightarrow$  channel) and  $4 \rightarrow 3$  (channel  $\rightarrow$  levee) transitions. This asymmetry, indicative of a relatively strong tendency for levee deposits to occur adjacently above channel deposits, was prescribed by the vertical transition probability data given shown in Figure 1. The fining-upward tendency is typical of fluvial deposition (Allen, 1970b) and is consistent with a Walther's Law interpretation of levee deposits tending to occur laterally adjacent to channel deposits (Allen, 1970a). Lesser asymmetries in the  $2 \rightarrow 3$ ,

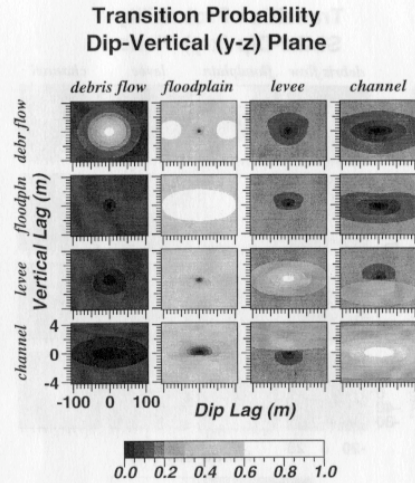


Figure 6. Slice from dip-vertical ( $y-z$ ) plane of a 3-D Markov chain model.

$3 \rightarrow 2$ ,  $2 \rightarrow 4$ , and  $4 \rightarrow 2$  transitions suggest a continuation of the fining-upward cycle to  $4 \rightarrow 3 \rightarrow 2$ , or channel  $\rightarrow$  levee  $\rightarrow$  floodplain, also evident by a conjugate pair of slightly complex eigenvalues in the vertical ( $z$ ) direction rate matrix.

The off-diagonal transition probabilities  $t_{1k}(h_x, 0, h_z)$  and  $t_{j1}(h_x, 0, h_z)$  associated with transitions to and from debris flows (category 1) show some asymmetry. However, no halo-like transition probability highs occur as in the  $3 \rightarrow 4$  and  $4 \rightarrow 3$  transitions in Figure 4, indicating relatively random juxtapositional relationships for debris flows. Note that in all entries of the transition matrix in Figure 4, the strike ( $x$ )-direction symmetry of  $t_{jk}(h_x, 0, h_z) = t_{jk}(h_{-x}, 0, h_z)$  persists, a condition that was enforced by (21) in the development of the strike ( $x$ )-direction model of Figure 2.

A slice through the strike-dip ( $x-y$ ) plane at  $h_z = 0$  shown in Figure 5 displays in  $t_{34}(h_x, h_y, 0)$  and  $t_{43}(h_x, h_y, 0)$  a tendency for levee deposits (category 3) to occur adjacent in the  $\pm$ strike ( $\pm x$ ) direction next to channel deposits (category 4), as expected according to a Walther's Law interpretation of a vertical fining-upward tendency. A slight tendency for debris flows to occur adjacent in the dip direction to floodplain deposits is evident in the  $t_{12}(h_x, h_y, 0)$  model, which could be attributed to better preservation potential for debris flows deposited in floodplain areas.

A slice through the dip-vertical ( $y-z$ ) plane at  $h_x = 0$  shown in Figure 6 again displays the strong vertical asymmetry evident in the  $3 \rightarrow 4$  and  $4 \rightarrow 3$  transitions because the levee deposits tend to occur adjacently above channel deposits. The tendency for debris flows to occur adjacently in the dip direction to floodplain deposits also is evident in the  $1 \rightarrow 2$  model. The model is symmetric in the  $y$  direction as enforced by (21) during conceptual development of the dip ( $y$ )-direction model shown in Figure 3.

Overall, the 3-D model displays some structures that appear ellipsoidal and others that are clearly nonellipsoidal when strongly asymmetric transition rates occur. The nonellipsoidal, vertically asymmetric characteristics of transition probability structures in Figures 4 and 6 are supported strongly by the data in Figure 1. It is difficult to conceive how the linear coregionalization approach typically used in geostatistics (e.g., Journel and Huijbregts, 1978, p. 171; Gouillard and Voltz, 1992; Goovaerts, 1994) could be used to build such three-dimensional, asymmetric, and nonellipsoidal structures into a coregionalization model. Yet, nonellipsoidal structures surely are needed to model asymmetric juxtapositional patterns in geology.

## CONCLUSIONS

A basic mathematical and conceptual understanding of the transition rate matrix is crucial to quantitative or subjective development of continuous-lag Markov chain models. Sylvester's theorem eases establishment of transition rate matrices, as well as calculation of transition probabilities for Markov chain models. Three-dimensional continuous-lag Markov chain models can be developed by interpolating transition rate matrices for 1-D continuous-lag Markov chain models established for three principal directions.

Given that 1-D Markov chain models have shown a long-standing applicability to geologic problems, 3-D continuous-lag Markov chain models also should prove useful to modern 3-D applications. Markov chain models can be developed either directly from exhaustive data, semiquantitatively through fitting of transition rates, or conceptually from geologic interpretations of proportions, mean lengths, elongation ratios, and juxtapositional tendencies. The conduciveness to conceptual development is important when faced with sparse or no data for quantifying spatial variability in certain directions, which often occurs in practical 2- and 3-D geologic applications.

Given that transition probabilities can formulate (co)kriging estimates (Carle and Fogg, 1996) and objective functions in simulated annealing (Deutsch and Journel, 1992, p. 159), Markov chain models also may be applied to geostatistical estimation and simulation techniques. Two- and 3-D continuous Markov chain models can address asymmetric heterogeneity patterns such as fitting-

upward tendencies that traditional geostatistical variogram models cannot. The emergence of 2- and 3-D continuous Markov chain models should encourage geostatistical approaches to tap into an extensive body of research and literature on geological applications of Markov chains.

#### ACKNOWLEDGMENTS

The paper was significantly improved by the comments of an anonymous reviewer. The authors further benefited from suggestions by E. M. LaBolle and D. VanBrocklin. This work was supported by grants from Lawrence Livermore National Laboratory, the U.S. Waterways Experimentation Station, N.I.E.H.S. Superfund Grant (ES-04699), U.S.G.S. Water Resources Research Grant (14-18-001-61909), and the U.S. EPA (R819658) Center for Ecological Health Research at UC Davis. Although the information in this document has been funded in part by the United States Environmental Protection Agency, it may not necessarily reflect the view of the Agency, and no official endorsement should be inferred.

#### REFERENCES

- Allen, J. R. L., 1970a, Studies in fluvial sedimentation: a comparison of fining upwards cyclothems with special reference to coarse-member composition and interpretation: *Jour. Sed. Pet.*, v. 40, no. 1, p. 298-323.
- Allen, J. R. L., 1970b, Physical processes of sedimentation: American Elsevier Publ. Co., New York, 248 p.
- Agterberg, F. P., 1974, *Geomathematics*: Elsevier Scientific Publ. Co., Amsterdam and New York, 596 p.
- Carle, 1996, A transition probability-based approach to geostatistical characterization of hydrostratigraphic architecture: unpubl. doctoral dissertation, Univ. California, Davis, 248 p.
- Carle, S. F., and Fogg, G. E., 1996, Transition probability-based indicator geostatistics: *Math. Geology*, v. 28, no. 4, p. 453-477.
- Carr, D. D., Horowitz, A., Hrarbar, S. V., Ridge, K. F., Rooney, R., Straw, W. T., Webb, W., and Potter, P. E., 1966, Stratigraphic sections, bedding sequences and random processes: *Science*, v. 28, no. 3753, p. 89-110.
- Dacey, M. F., and Krumbain, W. C., 1970, Markovian models in stratigraphic analysis: *Math. Geology*, v. 2, no. 2, p. 175-191.
- Deutsch, C. V., and Journel, A. G., 1992, *GSLIB: Geostatistical Software Library and user's guide*: Oxford Univ. Press, New York, 340 p.
- Doveton, J. H., 1971, An application of Markov chain analysis to the Ayrshire Coal Measures succession: *Scott. Jour. Geology*, v. 7, no. 1, p. 11-27.
- Doveton, J. H., 1994, Theory and applications of vertical variability measures from Markov chain analysis, in Yarus, J. H., and Chambers, R. L., eds., *Stochastic Modeling and Geostatistics: Computer Applications in Geology*, No. 3, Am. Assoc. Petroleum Geologists, Tulsa, Oklahoma, 379 p.
- Ethier, V. G., 1975, Application of Markov analysis to the Banff Formation (Mississippian), Alberta: *Math. Geology*, v. 7, no. 1, p. 47-61.
- Gingerich, P. D., 1969, Markov analysis of cyclic alluvial sediments: *Jour. Sed. Pet.*, v. 39, no. 1, p. 330-332.
- Goodman, L. A., 1968, The analysis of cross-classified data: independence, quasi-independence, and interaction in contingency table with and without missing entries: *Jour. Am. Stat. Assoc.*, v. 63, p. 1091-1131.
- Goovaerts, P., 1994, On a controversial method for modeling a coregionalization: *Math. Geology*, v. 26, no. 2, p. 197-204.
- Goulard, M., and Voltz, M., 1992, Linear coregionalization model: Tools for estimation and choice of cross-variogram matrix: *Math. Geology*, 24, no. 3, p. 269-286.
- Harbaugh, J. W., and Bonham-Carter, G. F., 1970, *Computer simulation in geology*: Wiley-Interscience, New York, 575 p.
- Hattori, I., 1976, Entropy in Markov chains and discrimination of cyclic patterns in lithologic successions: *Math. Geology*, v. 8, no. 4, p. 477-497.
- Journel, A. G., and Huijbregts, C. J., 1978, *Mining geostatistics*: Academic Press, London, 600 p.
- Krumbain, W. C., 1967, FORTRAN IV computer programs for Markov chain experiments in geology: *Kansas Geol. Survey, Computer Contr.* 38 p.
- Krumbain, W. C., 1968, FORTRAN IV computer program for simulation of transgression and regression with continuous-time Markov models: *Kansas Geol. Survey, Computer Contr.* 26, 38 p.
- Krumbain, W. C., and Dacey, M. F., 1969, Markov chains and embedded Markov chains in geology: *Math. Geology*, v. 1, no. 1, p. 79-96.
- Leeder, M. R., 1982, *Sedimentology*: George Allen & Unwin Ltd, London, 344 p.
- Lin, C., and Harbaugh, J. W., 1984, Graphic display of two- and three-dimensional Markov computer models in geology: *Van Nostrand Reinhold*, New York, 180 p.
- Miall, A. D., 1973, Markov chain analysis applied to an ancient alluvial plain succession: *Sedimentology*, v. 20, no. 3, p. 347-364.
- Miall, A. D., 1982, *Analysis of fluvial depositional systems: Education course notes series #20*: Am. Assoc. Petroleum Geologists, Tulsa, Oklahoma, 75 p.
- Moss, B. P., 1990, Stochastic reservoir description: a methodology, in Hurst, A., Lovell, A., and Morton, A. C., eds., *Geological applications of wireline logs*: *Geol. Soc. London Spec. Publ.*, v. 48, p. 57-75.
- Noyes, C. D., 1990, *Hydrostratigraphic analysis of the Pilot Remediation Test Area, LLNL, Livermore, California*: unpubl. masters thesis, Univ. California, Davis, 165 p.
- Politis, D. N., 1994, Markov chains in many dimensions: *Adv. Appl. Prob.*, v. 26, no. 3, p. 756-774.
- Potter, P. E., and Blakely, R. F., 1967, Generation of a synthetic vertical profile of a fluvial sandstone body: *Jour. Soc. Petr. Eng. of AIME*, v. 7, no. 3, p. 243-251.
- Press, W. H., Teukolsky, S. A., Vetterling, W. T., and Flannery, B. P., 1992, *Numerical recipes in FORTRAN*: Cambridge Univ. Press, New York, 963 p.
- Qualheim, B. J., 1988, Well log report for the LLNL ground water project 1984-1987, Lawrence Livermore National Laboratory, UCID-21342 (updated 1989 and 1993), 12 p plus 340 sheets.
- Rivoirard, J., 1994, *Introduction to disjunctive kriging and non-linear geostatistics*: Oxford Univ. Press, New York, 180 p.
- Rolke, W. A., 1991, Continuous-time Markov processes as a stochastic model for sedimentation: *Math. Geology*, v. 23, no. 3, p. 297-304.
- Ross, S., 1993, *Introduction to probability models (5th ed.)*: Academic Press, San Diego, California, 556 p.
- Schwarzacher, W., 1969, The use of Markov chains in the study of sedimentary cycles: *Math. Geology*, v. 12, no. 3, p. 213-234.

- Smith, B. T., Boyle, J. M., Dongarra, J. J., Garbow, B. S., Ikebe, Y., Klema, V. C., and Moler, C. B., 1976, Matrix eigensystem routines—EISPACK guide: Lecture notes in computer science (2nd ed.), v. 6: Springer-Verlag, New York, 551 p.
- Switzer, P., 1965, A random set process in the plane with a Markovian property (note): *Ann. Math. Stat.*, v. 36, no. 2, p. 1859-1863.
- Turk, G., 1982, Markov chains: Letters to the Editor: *Math. Geology*, v. 14, no. 5, p. 539-542.
- Turk, G., Naylor, M. A., and Woodcock, N. H., 1979, Transition analysis of structural sequences (discussion): *Geol. Soc. America Bull.*, v. 90, no. 10, 1989-1991.
- Vistelius, A. B., 1949, On the question of the mechanism of formation of strata: *Dokl. Akad. Nauk SSSR*, v. 65, no. 2, p. 191-194.
- Vistelius, A. B., 1967, *Studies in mathematical geology*: Consultants Bureau, New York, p. 252-258.